Within-Stand Boundary Effects of SWE Distribution in Forested Areas

R.W. Webb[1,2,3], M.S. Raleigh[4,5], D. McGrath[6], N.P. Molotch[2,7], K. Elder[8], C. Hiemstra[9], L. Brucker[10,11], and H.P. Marshall[12,13]

SnowEx Workshop 2019

Funding Provided by NASA
THP award #17-THP17-0060

Introduction

- Snow accumulation and melt vary with elevation, topography (e.g. aspect, slope), and canopy effects on wind redistribution and energy budgets
- Field and modeling studies on canopy-snow interactions have often been limited to the plot scale and binary in approach when considering forested areas (i.e. open vs. forest)
- Most studies have investigated open areas adjacent to forest stands and variability within the open areas but not so within forest stands.
- Within-stand snow water equivalent (SWE) distributions are often averaged with little quantitative focus in the transitional zones across stand boundaries (i.e. the edge of a forest stand canopy immediately adjacent to a clearing)
- There remains a gap in understanding the length scales of edge effects on SWE distribution for within-stand boundary areas (i.e. the transition from in clearing to under canopy SWE distribution patterns).
- Data from SnowEx provide opportunities to examine forest boundary effects on the SWE distribution in within-stand boundary areas.
- We define six distinct areas within and around a forest stand, defining the forest boundary as the edge between forest canopy and clearing to investigate in this study (Fig. 1).

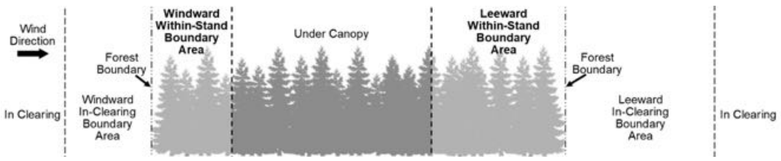

Figure 1. Defined areas as they pertain to a forest stand, it's boundary, and the dominant wind direction. The within-stand boundary areas of interest for this study are labeled in bold.

Research Goals & Questions

The goal of this study is to quantify the distance that the transition from in clearing to under canopy SWE distribution patterns occur. To accomplish this, we use a unique ground penetrating radar (GPR) dataset obtained during SnowEx17 on Grand Mesa, to assess the following research questions:

1) What are the distances from the forest boundary over which within-stand spatial patterns of SWE are affected (i.e. the extent of within-stand boundary areas in Fig.1)?
2) Is there a significant difference in SWE and distribution patterns in within-stand boundary areas relative to under canopy conditions?

Grand Mesa Study Site

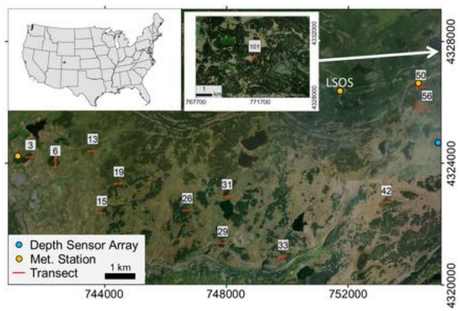

Figure 2. Overview of the Grand Mesa showing the transects surveyed with ground penetrating radar and analyzed in this study, meteorological station locations, and snow depth sensor array (Jennings et al., 2018).

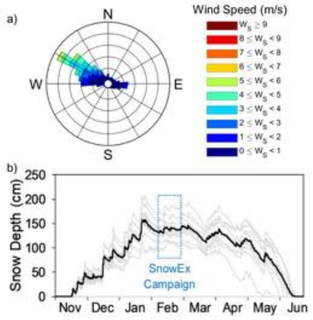

Figure 3. a) Wind rose for LSOS) and b) snow depth measurements from an acoustic sensor array with the black line showing the mean (Jennings et al., 2018).

Table 1. Transect orientation and stand description at location of each transect.

Transect ID	3	6	13	15	19	26	29	31	33	42	49	50	56	101
Transect Orientation	EW	NS	EW	EW	EW	EW	EW	EW	EW	EW	NS	EW	EW	EW
Stand Length (m)	230	420	55	275	150	605	235	135	30	70	565	620	335	540
Stand Width (m)	220	150	130	320	800	880	360	340	220	1310	850	635	1390	700
Avg Stand Height (m)	16.1	5.8	10.3	11.0	8.3	11.9	12.0	8.5	15.2	4.7	5.8	9.2	8.5	3.9

Methods

- Surveys were performed using a Mala Geosciences, Inc. ProEx GPR system with a 1.6 GHz shielded antenna fixed in place on a plastic sled
- The two-way traveltime (t) of the ground surface reflection was used to calculate snow depth (d_s) and estimate SWE based on density and velocity (v) observations at snow pit locations Fig. 4).

$$d_s = v * 0.5t$$

- Observations were made of variogram ranges over the entire transect and the coefficients of variation (COV) in a 50 m moving window to assess SWE variability.
- The length of within-stand boundary areas were determined using piecewise linear regression with a least squared approach and minimizing the slope after the breakpoint (representing background under canopy conditions (Fig. 5).
- The Wilcoxon rank-sum (a.k.a. Mann-Whitney) test was used to test for significant differences between under canopy and within-stand boundary areas for both COV and SWE values.

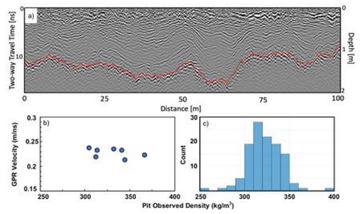

Figure 4. GPR data showing: a) an example radargram, b) mean density measurements from snow pits that were co-surveyed by the GPR to obtain radar wave velocity, and c) a histogram of all snow pit bulk density observations on Grand Mesa during SnowEx17 (Elder et al., 2018).

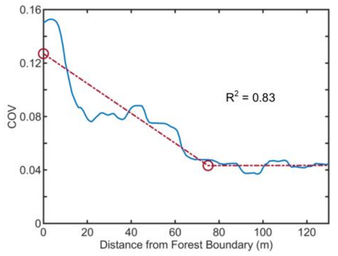

Figure 5. Example piecewise linear regression used to determine the length of the within stand boundary area.

Results

- COV generally decreased in forested areas (Fig. 6).
- The within-stand boundary areas were found to be (Fig. 7):
  - Windward: mean = 22 m (2.9 x canopy ht.), median = 25 m (2.3 x canopy ht.).
  - Leeward: mean = 44 m (4.2 x canopy ht.), median = 48 m (4.0 x canopy ht.).
- All within-stand boundary areas had significantly different COV values compared to under canopy conditions. For SWE values: 7 of 11 windward and 5 of 7 leeward within-stand boundary areas were significantly different than under canopy values.

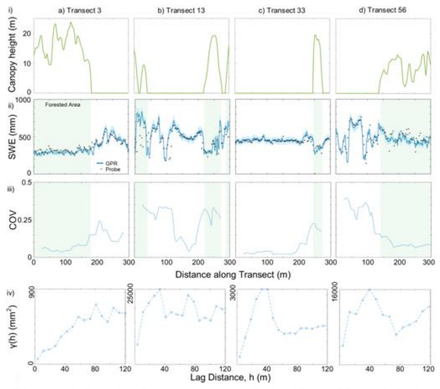

Figure 6. Results for transects: a) 3, b) 13, c) 33, and d) 56 showing i) canopy height (Painter et al., 2018), ii) SWE derived from GPR and 3 m spaced snow depth probe observations (Brucker et al., 2018), iii) SWE COV in a 50 m moving window, and iv) the variogram for the entire transect (note differences in y-axes). All data has been oriented such that wind direction is from left to right. Uncertainty bands in row (ii) were estimated using the range of observed bulk snow densities (Fig. 4) and estimated accuracy of GPR picks. SWE estimates using snow depth probes for row ii were calculated by multiplying depth by the nearest pit observed snow density in similar canopy condition.

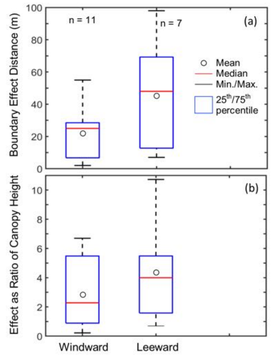

Figure 7. Boxplot summary of forest boundary effects for all windward and leeward within-stand boundary areas surveyed in the analyzed transects and presented as (a) distance from the forest boundary and (b) a ratio of mean stand canopy height.

Discussion & Conclusions

- We attribute much of this distribution to wind effects (Fig. 8)
  - Windward forest boundary will create an abrupt change in wind vectors
  - Effective roughness will decrease towards the leeward side of the stand and a recirculation region forms, altering the wind patterns in the leeward within-stand boundary area
- These dynamics will impact SWE distribution during snowfall events, redistribution of intercepted snow , and redistribution of deposited snow from in-clearing to forested areas.
- There is much work that could be done to further understand the complex fluid dynamics and how this relates to the redistribution of snow in a forested area.
  - Further investigation is also warranted at within-stand boundary areas that are: oriented parallel to wind direction, have less consistent wind directions, and consist of different canopy architectures.
- To quantify under canopy conditions in forested areas for model validation or survey designs, within-stand boundary areas are important to consider.

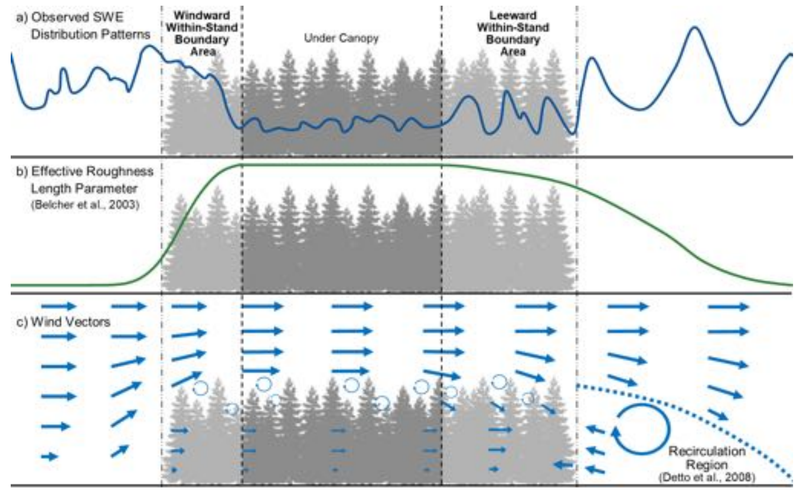

Figure 8. Conceptual diagram showing: a) SWE distribution observed using relative depths of transects 56 (windward side) and 3 (under canopy and leeward side) b) the relative effective roughness length parameter (Belcher et al., 2003), and c) expected wind vectors as a result of the effective roughness length parameter and recirculation region on the leeward edge of the stand (Detto et al., 2008)..

Acknowledgements

Funding for this work provided by NASA THP award #17-THP17-0060 and NSF EAR award #1624853 and NASA THP award #17-THP17-0060.

References

Jennings, K. S., T. B. Barnhart, and N. P. Molotch (2018), SnowEx17 Time Series Sonic Snow Depth Measurement Array, Version 1, edited by NASA NSIDC, Boulder, Colorado USA. 10.5067/5YJEYNLS1YK4.

Elder, K., L. Brucker, C. Hiemstra, and H. P. Marshall (2018), SnowEx17 Community Snow Pit Measurements, Version 1, edited by NASA NSIDC, Boulder, Colorado USA. doi: 10.5067/Q0310G10G1XULZS.

Webb, R. W., D. McGrath, K. Hale, and N. P. Molotch (2018), SnowEx17 Ground Penetrating Radar, Version 1, NSIDC, Boulder, Colorado. DOI: 10.5067/NPZYNEEGQUO.

Detto, M., G. Katul, M. Siqueira, J. Juang, and P. Stoy (2008), The structure of turbulence near a tall forest edge: The backward-facing step flow analogy revisited, Ecological Applications, 18(6), 1420-1435. doi: 10.1890/06-0920.1.

Belcher, S., N. Jerram, and J. Hunt (2003), Adjustment of a turbulent boundary layer to a canopy of roughness elements, Journal of Fluid Mechanics, 488, 369-398. doi: 10.1017/S0022112003005019.

Brucker, L., C. Hiemstra, H. P. Marshall, and K. Elder (2018), SnowEx Community Snow Depth Probe Measurements, Version 1, edited by NASA NSIDC, Boulder, Colorado USA. doi: 10.5067/WKC6VFMT7JTF.

Author Affiliations

[1]Department of Civil, Construction, & Environmental Engineering, University of New Mexico, Albuquerque, NM 87131.
[2]Institute of Arctic and Alpine Research, University of Colorado Boulder, Boulder, CO 80303 USA.
[3]Center for Water and the Environment, University of New Mexico, Albuquerque, NM 87131
[4]Department of Geological Sciences, University of Colorado Boulder, Boulder, CO 80303.
[5]National Snow and Ice Data Center, CIRES, University of Colorado Boulder, Boulder, CO 80303.
[6]Department of Geosciences, Colorado State University, Fort Collins, CO 80523.
[7]Department of Geography, University of Colorado Boulder, Boulder, CO 80303.
[8]Rocky Mountain Research Station, USDA Forest Service, Fort Collins, CO 80526
[9]U.S. Army Corps of Engineers, Cold Regions Research and Engineering Laboratory, Fort Wainwright, AK, USA 99703
[10]NASA Goddard Space Flight Center, Cryospheric Sciences Laboratory, Greenbelt, MD 20771 USA
[11]Universities Space Research Association, Goddard Earth Sciences Technology and Research Studies and Investigations, Columbia, MD 21046 USA
[12]Department of Geosciences, Boise State University, Boise, ID 83725.
[13]U.S. Army Corps of Engineers, Cold Regions Research and Engineering Laboratory, Hanover, NH 03755.